Journal of the Korean Society of Remote Sensing, Vol. 13, No.3, 1997, pp.265~276

Development of an Algorithm for Numerical Analysis of Wave Scattering from Sea Surfaces

Yi-Sok Oh

Dept. of Electronics and Electrical Engineering, Hong-Ik University, Seoul

바다에서의 전파 산란에 대한 수치적 해석 알고리즘 개발

오 이 석

홍익대학교 전자전기공학부

Abstract

Electromagnetic wave scattering from randomly rough sea surfaces was computed by using the Monte Carlo method and the Method of Moment. A relationship between the wind speed and the surface roughness parameters is obtained empirically at first. Then, a nonlinear directional randomly rough sea surface was generated for a given wind speed. This directional rough surface shows both vertical and horizontal skewness. An impedance boundary condition was used in the computation of the electric fields scattered from the nonlinear directional rough surfaces. A tapered impedance sheet was used to reduce the edge effect to improve the computation of the scattering coefficient at large incidence angles. It was shown that the computation result for sea surface scattering agreed well with the new PO model.

요 약

본 논문에서는 몬테카를로 방법과 모멘트법을 이용하여 불규칙적으로 거친 바다 표면에서의 전파 산란을 계산하였다. 우선, 풍속과 표면 거칠기 변수 사이의 관계식을 개략적으로 구하고, 풍속을 이용하여 비선형이며 방향성이 있는 불규칙적으로 거친 바다 표면을 생성하였다. 이 방향성이 있는 거친 표면은 수직적 편향성과 수직적 편향성을 모두 갖고 있다. 이 비선형적이고 방향성이 있는 거친 표면에서 산란

Received 10 November 1997 ; Accepted 30 November 1997.

된 전계를 계산하기 위해 임피던스 경계조건을 이용하였을 뿐만 아니라, 큰 입사각에서도 산란 계수를 정확하게 계산할 수 있도록 가장자리에 잘 만들어진 임피던스 조각을 사용하였다. 바다표면에 대한 수치해석 결과가 새로운 PO 모델과 잘 맞는 것을 보였다.

1. Introduction

Electromagnetic wave backscattering from a randomly rough sea surface driven by wind has been of interest in ocean remote sensing. Many experimental scatterometer data sets were obtained(Masuko et al, 1986; Li et al., 1989) and many theoretical models were introduced(Plant, 1986; Chen et al., 1992) for investigation of radar wave scattering from ocean surfaces. Numerical simulations were also introduced to get exact results of wave scattering from ocean surfaces(Fung and Chen, 1985; Johnson et al., 1998). Radar wave scattering from ocean surface, however, is not easy to handle because waves on the ocean are very complex. For example, the relation between wind speed and surface roughness is not clear yet.

In this paper, at first, a randomly rough sea surface was generated for a given wind speed. An approximate relationship between wind speed and rms surface height was obtained by using an empirical formula in Morchin(1993). The correlation length of a sea surface for a given wind speed was also obtained by using empirical formulas in Cox and Munk(1954) and Fung et al.(1989). Then, a randomly rough surface was generated by summation of random amplitude and phase, in which vertical skewness and horizontal skewness are included(Fung, 1994; Amar, 1989).

Electromagnetic wave scattering from the randomly rough sea surface generated as described above, was computed by the Method of Moment(MM) and Monte Carlo method. In this computation, an approximate boundary condition was used since the dielectric constant is large and the curvature is also large enough(Senior and Volakis, 1991), and a tapered impedance sheet was used to reduce the edge effect(Oh and Sarabandi, 1997).

2. Sea Surface Generation

A randomly rough surface can be generated by a convolutionary method(Fung et al., 1985) or by a superposition method(Amar, 1989) for given surface statistics. For sea surfaces, the parameters of surface statistics such as rms surface height and correlation length are dependent on wind speed. However, the relationship between the parameters and wind speed is not clearly defined yet. Therefore, an empirical formula for the relation is generated by a rule of thumb.

An empirical model for rms surface height was given by Morchin(1993) as follows;

$$\sigma \approx 0.025 + 0.046\, S_s^{1.72} \; or \approx H_3/4 \quad \text{.......} \quad (1)$$

where S_s is the sea state describing sea surface roughness according to the wind speed. The sea state defined by the World Meteorlogical Organization ranges from 0 to 9, *e.g.*, S_s=0 for calm, glassy sea (U=0-3 knots), S_s=1 for calm, rippled sea (U=4-6 knots), S_s=2 for smooth, wavelet-like sea (U=7-10 knots), S_s=3 for slightly rough sea (U=11-16 knots), S_s=4 for moderately rough sea (U=17-21 knots), etc. H_3 is the average value of the highest one-third of the wave. The sea states corresponding to wind speeds are shown in Fig. 1. The continuous line in Fig. 1 is obtained by data-fitting of discrete definition as follows;

$$S_s \approx \begin{cases} 0.432U, & U \leq 10.78 \\ 0.167U + 2.857, & U > 10.78 \end{cases} \quad \text{.......} \quad (2)$$

where U is wind speed in m/sec.

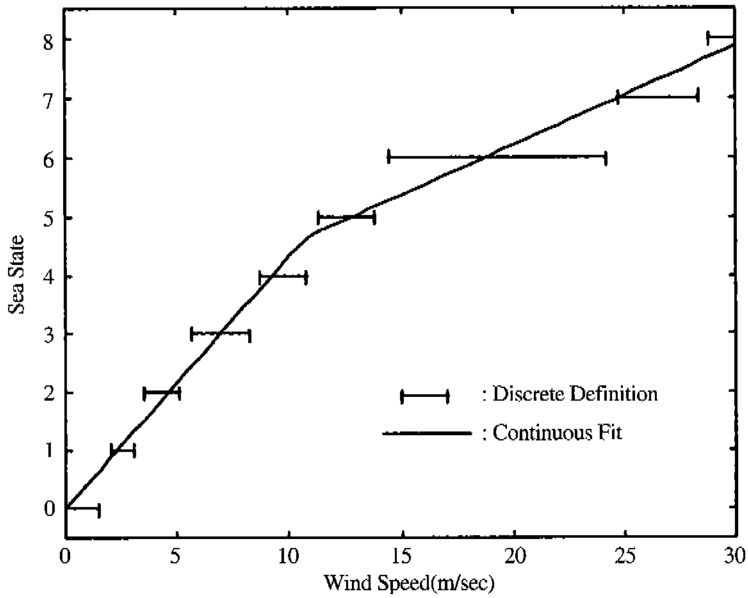

Figure 1. Relationship between the sea state and wind speed.

Equation (1) has two different forms as shown in Fig. 2, one as a function of S_s and the other of H_3.

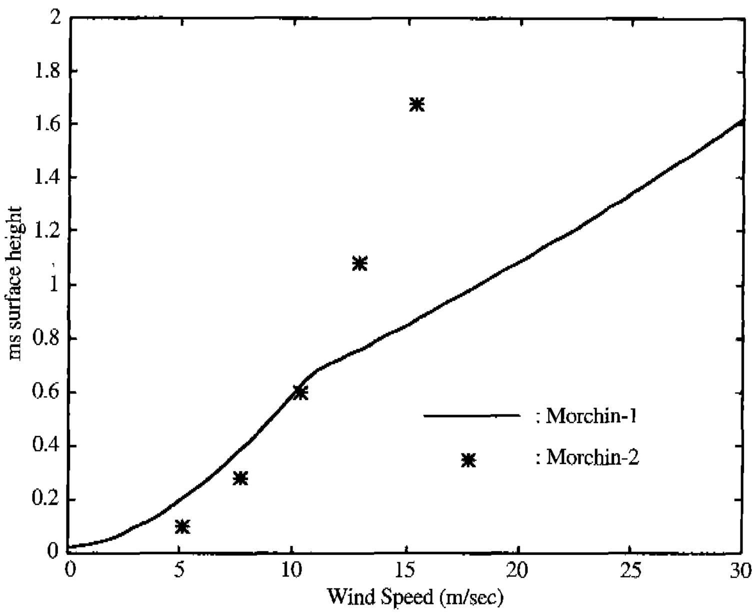

Figure 2. Relationship between rms surface height and wind speed.

The solid line in Fig. 2 represents the first part of (1) and is used in the computations of rms heights of sea surfaces.

According to Fung et al.(1989), the surface slope variances with respect to the upwind and cross-wind directions are related to the surface correlation lengths by

$$\sigma_u^2 \approx \frac{3\pi^2\sigma^2}{16\beta L_x^2} \quad \text{and} \quad \frac{3\pi^2\sigma^2}{16\beta L_y^2}, \qquad (3)$$

and the variances are also related to the wind speed as in Cox and Munk(1954) by

$$\sigma_u^2 = 0.00316U \quad \text{and} \quad \sigma_u^2 = 0.003+0.00192U, \qquad (4)$$

where $\beta = \pi^{2/3}/2$. The correlation length in upwind direction would be smaller to that in the crosswind direction, and (4) may be revised as $\sigma_u^2 = 0.003+0.00316U$. Then, the correlation lengths with respect to upwind and crosswind directions can be obtained from windspeed U and rms height σ as follows;

$$L_x \approx 3.41\sigma(0.003+0.00316U)^{-0.5}, \qquad (5)$$
$$L_x \approx 3.41\sigma(0.003+0.00192U)^{-0.5}.$$

Let $z(x,t)$ be any point on one-dimensional random directional sea surface. Then, $z(x,t)$ can be represented to the first order perturbation by the superposition of cosine waves with random amplitudes and random phases as follows(Longuet-Higgins, 1963; Amar, 1989);

$$z(x,t) = \sum_{m=1}^{M} a_m \cos(\psi_m) \qquad (6)$$

where $\psi_m = k_m x - \omega_m t + \phi_m$, k_m is the physical wavenumber measured in (rad/m), ω_m is the frequency such that $\omega_m^2 = gk_m$, where g is the gravitational acceleration in (m/sec^2). For the purpose of this work, time variations are not considered. ϕ_m, is a random phase in (rad) distributed uniformly between $[-\pi, \pi]$ and a_m is a random amplitude in (m) chosen such that the random variables $a_m \cos(\phi_m)$ and $a_m \sin(\phi_m)$ are independent and normally distributed. In addition, the mean-square of the random amplitude a_m satisfies the following conditions:

$$\sum_{k_m} \frac{1}{2} \langle a_m^2(k_m) \rangle = W(k)\Delta k \qquad (7)$$

where $W(k)$ is the roughness spectrum and $k_m \in [k-\Delta k/2, k+\Delta k/2]$. Above equation states that the random amplitudes that correspond to all wavenumbers within the grid element are such that the sum of their mean-squares is equal to the differential volume bounded by the spectrum sampled at a point within the grid element and multiplied by Δk. If each differential grid sample Δk contains one and only one wavenumber component, then the amplitude becomes (Fung, 1994)

$$a_m = \sqrt{2W(k_m)\,\Delta k_m}. \qquad (8)$$

Above equations can be used for generation of directional sea surface with Gaussian random processes. Some phenomena, however, show that the ocean surface exhibits a trend of skewness. The phenomena are a consequence of the nonlinearities often associated with ocean waves and these nonlinearities are of higher order statistics(Amar, 1989). The nonlinearity obtained by using Tayfun(1986)'s model resulted in a random surface whose crests are narrow and peaked, and whose troughs are long and flat. Such asymmetry in the vertical direction is referred to as vertical skewness. On the other hand, horizontal skewness can also occur in sea water, which is an asymmetry due to tilted crests in the horizontal direction. A modified model for nonlinear surfaces to accommodate both vertical and horizontal skewness is presented in Fung(1994) as follows;

$$z_1(x) = z + \frac{1}{2}\bar{k}[(z^2 - \tilde{z}^2) + 2z\tilde{z}] \qquad (9)$$

where z is given in (6), $\bar{k}$ is the mean wavenumber, $\bar{k} = m_1/m_0$, and the moments are $m_i = \int k^i W(k)dk$ where i=1,2, and $\tilde{z}(x) = \sum_{m=1}^{M} a_m \sin \psi_m$ In (9), the vertical and horizontal skewness are due to the $(z^2 - \tilde{z}^2)$ term and the $z\tilde{z}$ term, respectively.

A sea surface profile having a Gaussian-type height distribution has been generated for a relatively calm sea with a wind speed of 2 m/sec. The rms height and the correlation length for

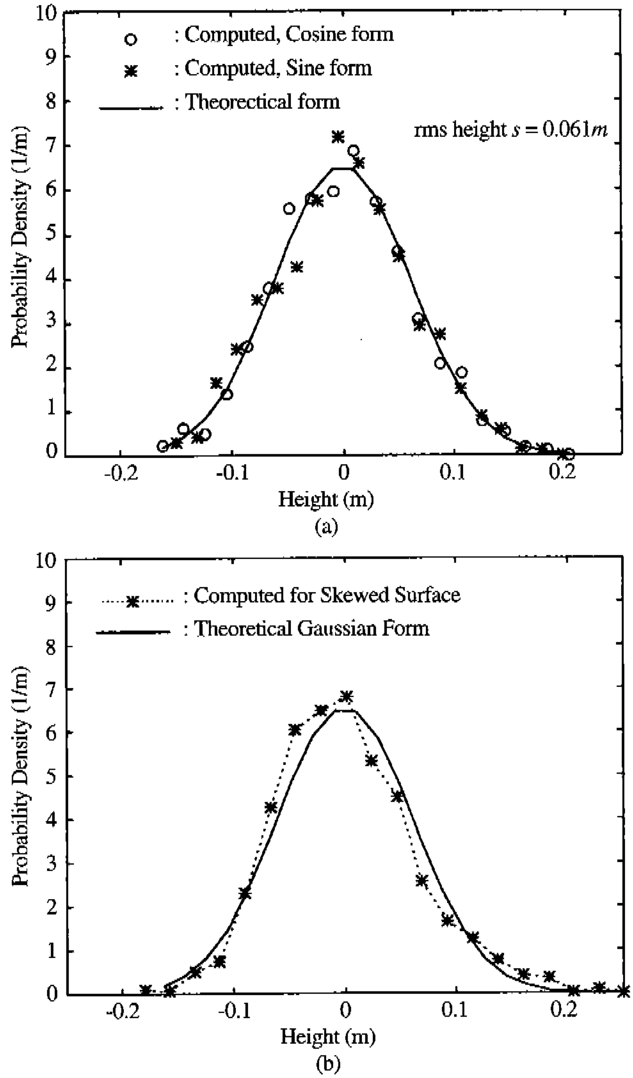

Figure 3. Probability density functions for (a) Gaussian-type surfaces and (b) a skewed surface.

the wind speed are approximately 0.061 m and 2.14 m, respectively. Figure 3 (a) shows that the probability density functions(pdf) of nonskewed height distributions z (cosine form) and $\tilde{z}$ (sine form) agree well with the Gaussian-type pdf with rms height of 0.061 m. The pdf of a skewed surface, however, has more points near the mean sea surface and is shifted to left because of horizontal and vertical skewness, respectively(Fung, 1994).

Figure 4(a) shows a vertically skewed profile compared with a nonskewed profile. The

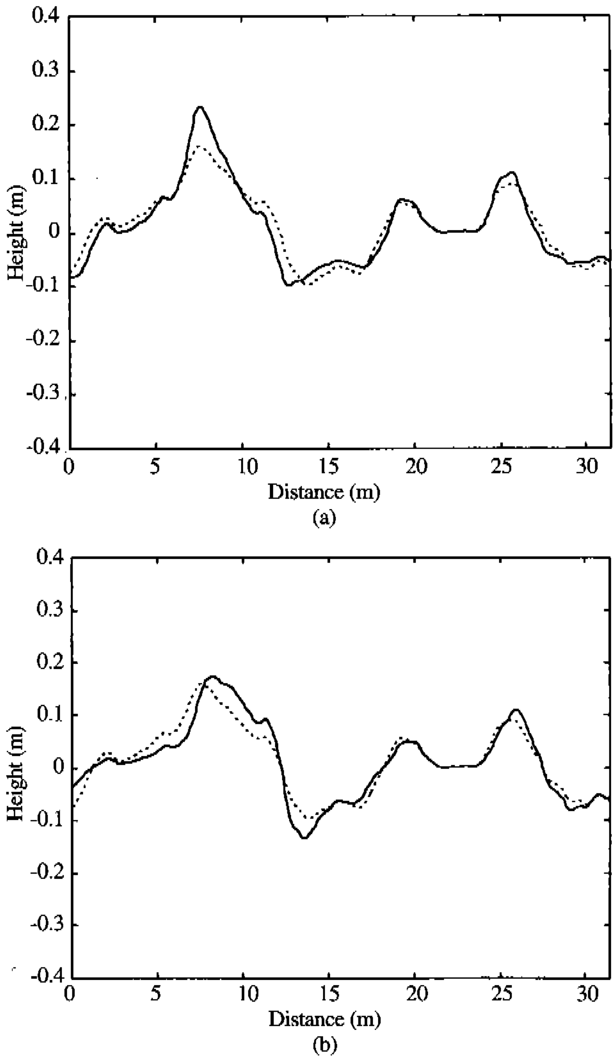

Figure 4. Sea surface profiles; (a) vertically skewed and (b) horizontally skewed surfaces.

vertically skewed profile has flattened troughs and narrower and larger peaks. This phenomena gives more points just below the mean sea surface in the pdf. Figure 4(b) shows a horizontally skewed sea surface profile. The crests are tilted in one direction and the troughs are tilted in the opposite direction.

The auto-correlation of the skewed profile agrees with a Gaussian-type function as well as the unskewed profiles. In this profile generation, total number of point N was 10001, the sampling rate Δk was 0.01 m^{-1}, and the sampling distance was 0.0628 m. The one-dimensional rough profile with horizontal and vertical skewness can be used for computing electric field scattered from the rough sea surface.

3. Scattering Coefficient Computation

Approximate boundary conditions can be very helpful in simplifying numerical computation of wave scattering. An impedance boundary condition in Cartesian coordinate system can be written as (Senior and Volakis, 1991)

$$\hat{n}\times(\hat{n}\times\overline{E}) = -\eta\hat{n}\times\overline{H} \quad \text{......} \quad (10)$$

where $\hat{n}$ is the unit vector normal in the outward direction. The parameter η is simply the intrinsic impedance of the material,

$$\eta = \sqrt{\frac{\mu_0\mu_r}{\varepsilon_0\varepsilon_r}},$$

which is valid for a curved surface under the conditions of

$$|N| \gg 1 \quad \text{and} \quad |\mathrm{Im}\, N|\, k_0\rho_l \gg 1, \quad \text{......} \quad (11)$$

where $N=\sqrt{\varepsilon_r\mu_r}$ is the complex refractive index, k_0 is free-space wavenumber, and ρ_l is the principal radii of curvature. For a perfectly conducting surface, $\eta = 0$ as required in (10).

The statistics of the scattered field from a one-dimensional rough surface is obtained by a Monte Carlo simulation. Basically scattered fields from a large number of randomly generated sample surfaces are computed numerically, and are used to estimate the backscattering coefficient of the random surface.

First, the surface current density **J** on each surface sample excited by a plane wave is determined using the method of moments (MoM). For a horizontally polarized wave the electric field integral equation (EFIE) is derived as

$$\bar{E}^i(\bar{\rho}) = -\bar{E}^s(\bar{\rho}) + \eta\hat{n}\times\bar{H}^s(\bar{\rho}) \qquad (12)$$

and for a vertically polarized wave the magnetic field integral equation (HFIE) is derived as

$$-\hat{n}\times\bar{H}^i(\bar{\rho}) = \hat{n}\times\bar{H}^s(\bar{\rho}) - \frac{1}{\eta}\bar{E}^s(\bar{\rho}) \qquad (13)$$

where (Oh; 1993)

$$\bar{E}^s(\bar{\rho}) = -\frac{k_0 Z_0}{4}\int_l \bar{J}(\bar{\rho}')H_0^{(1)}(k_0|\bar{\rho}-\bar{\rho}|)dl' \qquad (14)$$

$$\hat{n}\times\bar{H}^s(\bar{\rho}) = \frac{1}{2}\bar{J}(\bar{\rho}) + \frac{i k_0}{4}\int_l \bar{J}(\bar{\rho})(\hat{n}\cdot\hat{R})H_1^{(1)}(k_0|\bar{\rho}-\bar{\rho}'|)dl' \qquad (15)$$

and, $\hat{n} = \dfrac{-dz/dx\,\hat{x}+\hat{z}}{\sqrt{1+(dz/dx)^2}}$, $\hat{R} = \dfrac{\bar{\rho}-\bar{\rho}'}{|\bar{\rho}-\bar{\rho}'|}$.

Here Z_0 is the intrinsic impedance of free space, $H_0^{(1)}$ and $H_1^{(1)}$ are the zeroth and first order Hankel functions of the first kind, respectively. After a sample surface is discretized into sufficiently small cells, (12) and (13) are cast into matrix equations [**Z**][**I**] = [**V**], using pulse basis function and point matching technique. The elements of the impedance matrix [**Z**] can be computed by numerical integration of Hankel functions for off-diagonal elements and analytical approximation of the functions for diagonal elements (Oh and Sarabandi; 1997). The scattered field can be computed from the surface current by using (14-15) and the far-field approximation of the Hankel fuction (Oh, 1994).

The surface current induced by a horizontally polarized incidence wave exhibits the familiar singularity near the edges of the surface, which has a significant effect on the backscattered field away from normal incidence. However, this is not the case for the vertically polarized incidence wave for a one-dimensional surface. To suppress the peak current near the edges a tapered impedance sheet is added to each end of the surface sample. The impedance profile $\eta_{tr}(x)+i\eta_{ti}(x)$ can be given as a function of position near the edges with smoothly tapered values, which plays an important role in suppression of the edge current. Using trial and error the following impedance profile was chosen:

$$\eta_{tr}(x) + i\eta_{ti}(x) = \eta_r + i\eta_i, \quad |x|\le\frac{D}{2}$$

$$\eta_{tr}(x) = Z_0\left[\frac{|x|-D/2}{D_I}\right]^4 + \eta_r, \quad \frac{D}{2}\le|x|\le\frac{D}{2}+D_I \qquad (16)$$

$$\eta_{ti}(x) = \eta_i - \eta_i\left[\frac{|x|-D/2}{D_I}\right]^4, \quad \frac{D}{2}\le|x|\le\frac{D}{2}+D_I$$

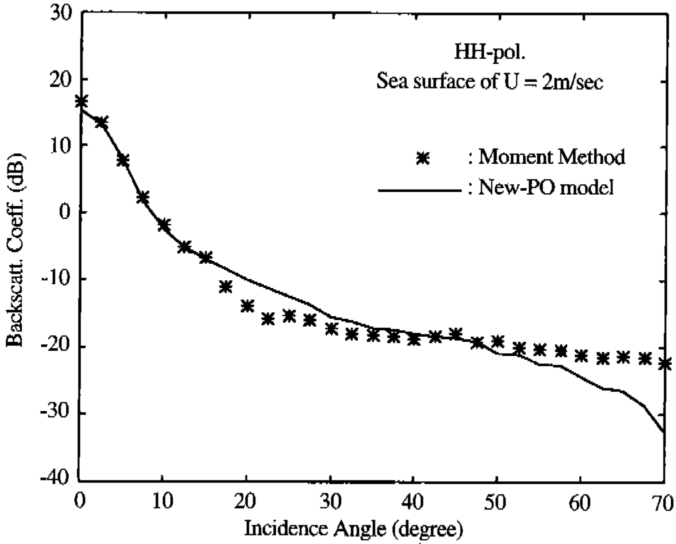

Figure 5. Comparison of numerical results with the new-PO model.

where D is the width of the sample surface and D_I is the width of the tapered impedance section at both sides.

The dielectric constant of sea water can be computed by a revised Debye formula given in (Ulaby et al., 1986), and ε_r = (71.6, 70.6) is obtained at 1.25GHz for the salinity of 30 $^0/_{00}$. The dielectric constant can be measured by a dielectric probe(Kim and Oh, 1997). The algorithm was applied to the surface which was generated according to the procedure in the previous section with vertical and horizontal skewness for wind speed of 2 m/sec at HH-polarization.

Figure 5 shows that the backscattering coefficients computed numerically by the algorithm agrees well with those computed by the new-PO model. The new-PO model is a theoretical model for random surface scattering, which is good for rough surface of $m<0.25$ where m is the rms surface slope (Oh, 1996). Because the rms slope of the surface is 0.04, the roughness of the surface is in the validity region of the new-PO model.

4. Conclusion

An algorithm for numerical computation of backscattering coefficient for sea surfaces is developed in this paper. A sea surface with vertical and horizontal skewness is generated by superposition of perturbed sinusoidal waves. Functional forms of surface parameters, rms surface height and surface correlation length, as functions of wind speed are formulated empirically. The scattered field of each surface segment is computed by the Method of Moment with implementation of the impedance boundary conditions. The numerical computation became much simpler by using the impedance boundary conditions. The backscattering coefficient of a sea surface was computed by the Monte Carlo method with the statistics of the scattered fields for all segments. It was shown that the backscattering coefficient computed by the algorithm agrees well with the new-PO model at the validity region of the theoretical model. Numerical computations for many more different types of sea surfaces may be needed for examining the effect of wind speed, direction, salinity, radar polarization, incidence angle, and frequency.

Acknowledgement: This work was supported in part by the Agency for Defense Development of Korea.

References

Amar, F., 1989, *Directional random sea surface generation,* MS thesis, Univ. of Texas at Arlington.

Chen, K.S., A.K. Fung, and D.E. Weissman, 1992, "A backscattering model for ocean surface", *IEEE Trans. Geoscience Remote Sensing,* 30(4) :811-817.

Cox, C., and W. Munk, 1954, "Measurement of the roughness of the sea surface from photographs of the sun's glitter", J. Opt. Soc. Am., 44(11) :838-850.

Fung, A.K. and M.F. Chen, 1985, "Numerical simulation of scattering from simple and composite random surfaces", *J. Opt. Soc. Am. A* 2(12) :2274-2284.

Fung, A.K., K.S. Chen, and M.F. Chen, 1989, "A note on the directional sea spectrum", *Remote Sens. Environ.,* 30 :95-106.

Fung, A.K., 1994, Micowave Scattering and Emission *Models and their Application,* Artech House

Jonson, J.T., R.T. Shin, J.A. Kong, L. Tsang, 1998, "A numerical study of the composite surface model for ocean backscattering", *IEEE Trans. Geoscience Remote Sensing,* 36(1) :72-83.

Kim, T. and Y. Oh, 1997, "Retrieval of soil moisture using microwave reflection at the end of a coaxial probe", *Journal of the Korean Society of Remote Sensing,* 13(2) (in Korean).

Li, F., W. Large, W. Shaw, E.J. Walsh, and K. Davidson, 1989, "Ocean radar backscatter relationship with near-surface winds: A case study during FASINEX", *J. Physical Oceanography,* 19 :342-353.

Longuet-Higgins, M.S., 1963, "The effect of non-linearities on statistical distributions in the theory of sea waves", Journal of Fluid Mechanics, 17(part.3) :459-480.

Masuko, H., K. Okamoto, M. Shimada, and S. Niwa, 1986, "Measurement of microwave backscattering signature of the ocean surface using X and Ka band airborne scatterometers, *J. Geophysical Research*, 91(C11) :13065-13083.

Morchin, W., 1993, *Radar Engineer's Sourcebook*, p.72-74, Artech House.

Oh, Y., 1993, *Microwave Polarimetric Backscattering from Natural Rough Surfaces*, Ph.D. Thesis, University of Michigan, Ann Arbor.

Oh, Y., 1994, "A semi-empirical model for microwave polarimetric radar backscattering from bare soil surfaces", *Journal of Korean Society of Remote Sensing*, 10(2) :17-36.

Oh, Y., 1996, "An exact evaluation of Kirchhoff approximation for backscattering from a one-dimensional rough surface", *IEEE AP-S International Symposium*, Baltimore, 3 :1522-1525.

Oh, Y. and K. Sarabandi, 1997, "Improved numerical simulation of electromagnetic wave scattering from perfectly conducting random surface", IEE Proc.-Microwave Antennas Propag., 144(4) :256-260.

Plant, W., 1986, "A two-scale model of short wind-generated waves and scatterometry", *J. Geophysical Research*, 91(C9) :10735-10749.

Senior, T.B.A. and J.L. Volakis, 1991, "Generalized impedance boundary conditions in scattering", Proceeding IEEE, 79(10) :1413-1420.

Tayfun, M.A., 1986, "On narrow-band representation of ocean waves; 1. Theory, 2. Simulations", J. Geophysical Res., 91(C6) :7743-7759.

Ulaby, F.T, Moore, M.K. and Fung, A.K., 1986, *Microwave Remote Sensing, Active and Passive*, vol. 2 and 3, Artech House, Norwood, MA.